AIAA JOURNAL
Vol. 31, No. 9, September 1993

Stability of Fluttered Panels Subjected to In-Plane Harmonic Forces

T. H. Young* and F. Y. Chen†
National Taiwan Institute of Technology, Taipei, Taiwan 10772, Republic of China

This paper presents an investigation into the stability of a fluttered panel acted on by an in-plane harmonic force. The in-plane force is assumed to be slow varying and small in magnitude compared to the aerodynamic force. Because of this small harmonic force, the system may become stable although the aerodynamic force exceeds its critical value. In this work, the finite element formulation is applied to obtain the discretized system equations. The autonomous terms in the system equations are then uncoupled by transforming these terms into Jordan canonical forms. Finally, the method of multiple scales is used to solve for analytical solutions of the system. The effects of system parameters on the changes of stability boundaries are studied numerically.

I. Introduction

THE stability behavior of elastic structures exposed in air is one of the major considerations in structural design, especially for aerospace structures where the minimum weight is one of its design goals. Therefore, hundreds of references regarding this topic can be found in the existing literature.[1,2] Most of the references consider panels subjected to aerodynamic forces only and deal primarily with the determination of the critical value of the aerodynamic pressure.

Durvasula[3] utilized the assumed mode method to calculate the critical aerodynamic pressure of a skew plate simply supported all around. In this paper, the aerodynamic damping term is neglected. Numerical results show that the critical value increases with increasing skew angle of the plate at aspect ratio equal to 1 and 2, and this value is the smallest at 15-deg skew angle when the aspect ratio is 1/2. The critical aerodynamic pressure of a quadrilateral plate was determined by Srinivasan and Babu.[4] Numerical results for plates with different boundary conditions are given. Olson[5] applied rectangular conforming and nonconforming elements and triangular conforming elements to find the critical aerodynamic pressure of square panels and delta wings. Convergence studies are presented for these three kinds of elements. It is observed that the results obtained by using conforming elements converge faster and are more accurate.

However, it would be more general and physically realistic to consider panels subjected to other forms of forces simultaneously, such as in-plane forces which may arise from internal pressurization[2] or local vibration of the surface panels.[6] Dugundji[7] found the exact solution of a simply supported rectangular plate subjected to both aerodynamic and in-plane forces. Numerical results show that the critical aerodynamic pressure increases with increasing aerodynamic and structural damping, especially at low aspect ratios. The critical aerodynamic pressure of a quadrilateral plate subjected simultaneously to in-plane loads was calculated by Sander et al.[8] by using conforming and nonconforming finite elements. In this work, convergence studies for these two kinds of elements and the effects of aspect ratio, flow angularity, and in-plane loads are presented, and the calculated results are also compared with experimental data. The in-plane force considered in the cited references is static. However, in real situations, the in-plane force is usually time dependent. Young and Chen[9] investigated the stability of skew plates subjected to both aerodynamic and in-plane oscillating forces. The aerodynamic force considered in this paper is smaller than its critical value. The authors find that with a small in-plane harmonic force, the plate may become unstable before the aerodynamic pressure reaches its critical value.

As for the subject of the stability of fluttered structures acted on by parametric excitation, only the papers by Fu and Nemat-Nasser[10,11] can be found in the literature. In these two papers, the stability of beams subjected to a transverse follower force and a perturbation of the force is studied by using a perturbation method. The stability boundaries of the combination resonances of the summed and difference types are derived. However, the case where the perturbation frequency is near zero is not discussed, which is very important practically for fluttered panels due to aerodynamic forces.

This paper presents an investigation into the stability of a panel subjected to an aerodynamic force with the magnitude exceeding its critical value and acted on simultaneously by an in-plane harmonic force. The panel is modeled as a cantilever skew plate and the in-plane harmonic force may be induced by the bending vibration of the frame structure onto which the panel is riveted. Usually, this kind of exciting force is small in magnitude and low in frequency.

II. Equation of Motion

A skew plate of side length $a \times b$ with a skew angle θ subjected to an air flow in the ζ_2 direction and an in-plane harmonic force $F \cos \Omega t$, where Ω is the exciting frequency in the ζ_1 direction, is shown in Fig. 1. In this figure, the relations between the skew coordinates (ζ_1, ζ_2) and the Cartesian coordinates (x_1, x_2) are given by

$$\zeta_1 = x_1 - x_2 \tan\theta \qquad \zeta_2 = x_2/\cos\theta \tag{1}$$

The aerodynamic pressure for sufficiently high supersonic flow can be described by the two-dimensional first-order theory (also called the piston theory) as[2]

$$p(x_1, x_2, t) = -\frac{2q}{\sqrt{M_\infty^2 - 1}}\left(\frac{\partial w}{\partial \zeta_2} + \frac{\dot{w}}{V}\frac{M_\infty^2 - 2}{M_\infty^2 - 1}\right) \tag{2}$$

where q is the dynamic pressure, M_∞ the Mach number, V the flow velocity, and w the transverse displacement; the overdot denotes a partial derivative with respect to time t. Therefore, for a thin plate with small deformation assumption, the equa-

Received April 1, 1992; revision received Sept. 15, 1992; accepted for publication Sept. 15, 1992.

*Associate Professor, Department of Mechanical Engineering.
†Graduate Research Assistant, Department of Mechanical Engineering.

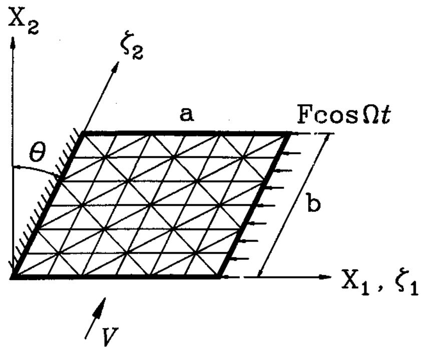

Fig. 1 Configuration and finite element discretization of a skew plate subjected to both aerodynamic and in-plane harmonic forces.

tion of motion of the plate subjected to both aerodynamic and in-plane forces can be written as

$$\rho h\ddot{w} + D\nabla^4 w + \left(\beta\frac{\partial w}{\partial \zeta_2} + \mu\dot{w}\right) + F\cos\Omega t\frac{\partial^2 w}{\partial \zeta_1^2} = 0 \quad (3)$$

where ρ, h, and D are the mass density, thickness, and flexural rigidity of the plate, respectively. In Eq. (3), ∇^4 denotes the biharmonic operator, and the aerodynamic pressure and damping parameters are

$$\beta = 2q/\sqrt{M_\infty^2 - 1}$$

and

$$\mu = (\beta/V)[(M_\infty^2 - 2)/(M_\infty^2 - 1)]$$

Equation (3) possesses no exact solutions; therefore, approximate methods must be utilized to find an approximate solution. In this paper, the finite element method is first used to get rid of the dependence on the spatial coordinates. By the use of the three-node triangular Cheung-Zienkiewicz-King (CZK) element,[12] the displacement within an element can be expressed as

$$w = N^T a_e \quad (4)$$

where the column matrices for the shape function and the nodal parameter N and a_e are given in Zienkiewicz.[12] Introduce the dimensionless variables and parameters defined as

$$\hat{a}_e = a_e/h, \quad \hat{t} = \sqrt{D/\rho h a^4}\,t, \quad \hat{\mu} = \mu a^2/\sqrt{\rho h D}$$

$$\hat{\beta} = \beta a^3/D, \quad \hat{F} = Fa^2/D, \quad \hat{\Omega} = \Omega\sqrt{\rho h a^4/D}$$

Substituting Eq. (4) into Eq. (3) and going through the finite element formulations yields the following equation for the discretized system:

$$[M]\hat{a}'' + \hat{\mu}[C]\hat{a}' + [K]\hat{a} + \hat{\beta}[F_p]\hat{a} + \hat{F}\cos\hat{\Omega}\hat{t}[F_i]\hat{a} = \mathbf{0} \quad (5)$$

where $[M]$, $[C]$, and $[K]$ are the mass, damping, and stiffness matrices, respectively; $[F_i]$ and $[F_p]$ are the force matrices due to the in-plane and aerodynamic forces, respectively; $\hat{a}$ is the column matrix formed by all the $\hat{a}_e$. In Eq. (5), the prime denotes a partial derivative with respect to $\hat{t}$. Note that the damping matrix $[C]$ is equal to the mass matrix $[M]$, and the matrices $[M]$ and $[K]$ are symmetric. In addition, the force matrix $[F_i]$ is symmetric if the line of action of the in-plane force remains unchanged.

Equation (5) is a set of simultaneous differential equations with variable coefficients and still cannot be solved exactly. To improve the solvability of the system equations, a modal analysis procedure is then applied to decouple all of the autonomous terms in the equations. The procedure is stated briefly as follows: First considering the corresponding undamped, autonomous system equations and assuming $\hat{a} = be^{i\omega\hat{t}}$ gives the following eigenvalue problem:

$$\omega^2[M]b - ([K] + \hat{\beta}[F_p])b = 0 \quad (6)$$

This equation can be solved for all the nondimensional natural frequencies ω and modal vectors b. For small values of $\hat{\beta}$, the natural frequencies are all real and distinct. As the value of $\hat{\beta}$ reaches a specific value, two of the natural frequencies become equal, and the system is said to be fluttered. This specific value of $\hat{\beta}$ is called the critical aerodynamic pressure (denoted $\hat{\beta}_{cr}$). In this work, $\hat{\beta} \geq \hat{\beta}_{cr}$ is assumed.

As $\hat{\beta}$ reaches $\hat{\beta}_{cr}$, the natural frequencies of the modes involved in flutter become equal, say $\omega_1 = \omega_2$, and the corresponding eigenvectors coalesce into one, i.e., $b_1 = b_2$. If another principal vector $b_2^*(b_2^* \neq b_2)$ (Ref. 13) corresponding to ω_1 can be found, one may form a "generalized modal matrix" to transform the matrices in the eigenvalue problem into their Jordan canonical forms. Before doing this, one must transform the generalized eigenvalue problem into a standard one first. A direct way of doing so is to calculate the inverse of the mass matrix $[M]^{-1}$ and then premultiply $[M]^{-1}$ with Eq. (6). However, to avoid numerical errors when inverting the mass matrix, a different procedure is adopted. The procedure consists of the following steps:

1) Solve the generalized eigenvalue problem of the corresponding natural system, i.e., $\lambda[M]d = [K]d$, to obtain the eigenvalues $\lambda_1, \lambda_2, \ldots, \lambda_N$ and eigenvectors $d_1, d_2, \ldots, d_N$, where N is the total number of degrees of freedom in the finite element formulation.

2) Introduce a linear transformation $e = [D]b$, where $[D]$ is a modal matrix formed by all the eigenvectors d_i normalized with respect to the mass matrix.

3) By the standard modal analysis procedure,[14] Eq. (6), after replacing $\hat{\beta}$ by $\hat{\beta}_{cr}$, becomes

$$\omega^2[I]e = ([\hat{K}] + \hat{\beta}_{cr}[\hat{F}_p])e \quad (7)$$

where $[\hat{K}]$ is a diagonal matrix with each diagonal entry being the eigenvalues λ_i, $i = 1, 2, \ldots, N$, and the matrix $[\hat{F}_p] = [D]^T[F_p][D]$ ($[D]^T$ is the transpose of $[D]$). Equation (7) is now a standard eigenvalue problem that may be solved for the eigenvalue ω^2 and the principal vector e. Note that all of the principal vectors e_i are distinct.

Now we are ready to uncouple the autonomous terms in Eq. (5). Introduce another linear transformation $\hat{a} = [D][E]y$, where $[E]$ is a principal matrix formed by all of the principal vectors e_i. Substituting this transformation into Eq. (5), premultiplying $[E]^{-1}[D]^T$ with this equation, and making use of orthogonality of the eigenvectors, yields the following equation:

$$y'' = \hat{\mu}y' + [J]y + (\hat{\beta} - \hat{\beta}_{cr})[G]y + \hat{F}\cos\hat{\Omega}\hat{t}[F]y = 0 \quad (8)$$

where the matrices

$$[F] = [E]^{-1}[D]^T[F_i][D][E]$$

and

$$[G] = [E]^{-1}[D]^T[F_p][D][E]$$

The matrix $[J]$ is in its Jordan canonical form

$$[J] = \begin{bmatrix} \omega_1^2 & 0 & 0 \cdots 0 \\ 1 & \omega_1^2 & 0 \cdots 0 \\ 0 & 0 & \omega_3^2 \cdots 0 \\ & & \cdots \\ 0 & 0 & 0 \cdots \omega_N^2 \end{bmatrix}$$

Equation (8) represents a partially uncoupled set of simultaneous equations that may be solved analytically in the case of weakly nonautonomous systems. To have a better insight into the solutions of the equations, a perturbation method is applied to obtain analytical solutions instead of direct integration of the equations numerically.

III. Perturbation Analysis

In this paper, the amplitude of the in-plane harmonic force $\hat{F}\cos\hat{\Omega}\hat{t}$ is assumed to be small compared to the aerodynamic force $\hat{\beta}$. Therefore, the small parameter ϵ appearing in the perturbation technique is defined as $\epsilon = \hat{F}/\hat{\beta}_{cr}$ in this investigation. In addition, let $\hat{\beta}$ be of the form

$$\hat{\beta} = \hat{\beta}_{cr}(1 + \kappa\epsilon + \cdots +) \tag{9}$$

where κ is a constant. Equation (8) can be rewritten as

$$y_2'' + \hat{\mu}y_2' + \omega_1^2 y_2 + y_1 = -\epsilon\hat{\beta}_{cr}\sum_{n=1}^{N}(\kappa g_{2n} + f_{2n}\cos\hat{\Omega}\hat{t})y_n + \mathcal{O}(\epsilon^2)$$

$$y_m'' + \hat{\mu}y_m' + \omega_m^2 y_m = -\epsilon\hat{\beta}_{cr}\sum_{n=1}^{N}(\kappa g_{mn} + f_{mn}\cos\hat{\Omega}\hat{t})y_n + \mathcal{O}(\epsilon^2)$$

$$m = 1, 2, \ldots, N, \qquad m \neq 2 \tag{10}$$

where y_m, f_{mn}, and g_{mn} are entries of the matrices y, $[F]$, and $[G]$, respectively.

In the present work, the method of multiple scales is used to find the solutions of Eq. (10). One begins by introducing the various time scales $T_j = \epsilon^{j\alpha_1}\hat{t}$, $j = 0, 1, 2, \ldots$, where α_1 is a constant to be determined. It follows that the derivatives with respect to $\hat{t}$ become expressions in terms of the partial derivatives with respect to T_j. Although the parametric excitation might stabilize the motion, one still expects the amplitude of y_2 to be much larger than that of y_1 (Ref. 15). Without loss of generality, the dependent variables are scaled as $y_m = \epsilon^{-\gamma_m}z_m$, where the z_m are of order 1, and the γ_m are positive constants to be determined in the solution except γ_1 which is set to 0. It is assumed that the variables z_m can be represented by a uniformly valid expansion having the form

$$z_m = z_{m0}(T_0, T_1, T_2) + \epsilon^{\alpha_1}z_{m1}(T_0, T_1, T_2) + \epsilon^{2\alpha_1}z_{m2}(T_0, T_1, T_2) + \cdots + \tag{11}$$

In addition, the in-plane force is assumed to be slow varying in this work. Hence, assume $\hat{\Omega} = 2\epsilon^{\alpha_2}\sigma$, where σ is a detuning parameter, and α_2 is also a constant to be determined. Substituting Eq. (11) into Eq. (10) yields

$$D_0^2 z_{m0} + \omega_m^2 z_{m0} + \epsilon^{\alpha_1}(D_0^2 z_{m1} + \omega_m^2 z_{m1} + 2D_0D_1z_{m0})$$
$$+ \epsilon^{2\alpha_1}(D_0^2 z_{m2} + \omega_m^2 z_{m2} 2D_0D_2z_{m0} + D_1^2 z_{m0} + 2D_0D_1z_{m1})$$
$$+ \epsilon^{\alpha_3}\tilde{\mu}[D_0z_{m0} + \epsilon^{\alpha_1}(D_0z_{m1} + D_1z_{m0})]$$
$$+ \epsilon^{1+\gamma_m}\hat{\beta}_{cr}\sum_{n=1}^{N}(\kappa g_{mn} + f_{mn}\cos 2\epsilon^{\alpha_2}\sigma T_0)\cdot\epsilon^{-\gamma_n}(z_{n0} + \epsilon^{\alpha_1}z_{n1} + \epsilon^{2\alpha_1}z_{n2}) = 0$$

$$m = 1, \ldots, N, \qquad m \neq 2 \tag{12a}$$

$$D_0^2 z_{20} + \omega_1^2 z_{20} + \epsilon^{\gamma_2}z_{10} + \epsilon^{\alpha_1}(D_0^2 z_{21} + \omega_1^2 z_{21} + \epsilon^{\gamma_2}z_{11} + 2D_0D_1z_{20})$$
$$+ \epsilon^{2\alpha_1}(D_0^2 z_{22} + \omega_1^2 z_{22} + \epsilon^{\gamma_2}z_{12} + 2D_0D_2z_{20} + D_1^2 z_{20} + 2D_0D_1z_{21}) + \epsilon^{\alpha_3}\tilde{\mu}[D_0z_{20} + \epsilon^{\alpha_1}(D_0z_{21} + D_1z_{20})]$$
$$+ \epsilon^{1+\gamma_2}\hat{\beta}_{cr}\sum_{n=1}^{N}(\kappa g_{2n} + f_{2n}\cos 2\epsilon^{\alpha_2}\sigma T_0)\cdot\epsilon^{-\gamma_n}(z_{n0} + \epsilon^{\alpha_1}z_{n1} + \epsilon^{2\alpha_1}z_{n2}) = 0 \tag{12b}$$

where $\hat{\mu} = \epsilon^{\alpha_3}\tilde{\mu}$ is assumed, and the differential operators $D_j = \partial/\partial T_j$.

To determine the effects of the excitation and the repeated frequency, one must at least include the term of $f_{12}z_{20}$ in Eq. (12a) and the term of z_{10} in Eq. (12b). Thus $\gamma_2 = \alpha_1 = ½$ are set. Moreover, since the first excitation term appears in the order of $\epsilon^{½}$, to have $\hat{\Omega}$ having time scale T_1 and have the damping term appearing in the same order with the first excitation term, $\alpha_2 = \alpha_3 = ½$ are assumed. In this case, all of the other γ_m cannot be determined unless initial conditions are taken into consideration. However, it can be easily shown that the stability of the motion is independent of the values of these γ_m. Therefore, these γ_m are set to zero for simplicity, i.e., $\gamma_m = 0$, for $m \geq 3$. In sum,

$$T_j = \epsilon^{j/2}\hat{t}, \qquad j = 0, 1, 2, \ldots$$
$$\hat{\Omega} = 2\epsilon^{½}\sigma$$
$$\hat{\mu} = \epsilon^{½}\tilde{\mu} \tag{13}$$
$$y_2 = \epsilon^{-½}z_2, \qquad y_m = z_m, \qquad \text{for} \quad m \neq 2$$

Equating the coefficients of like power of ϵ in Eq. (12) leads to the following equations:

Order 1

$$D_0^2 z_{20} + \omega_1^2 z_{20} = 0$$
$$D_0^2 z_{m0} + \omega_m^2 z_{m0} = 0 \qquad \text{for } m \pm 2 \tag{14}$$

Order $\epsilon^{½}$

$$D_0^2 z_{21} + \omega_1^2 z_{21} = -2D_0D_1z_{20} - \tilde{\mu}D_0z_{20} - z_{10}$$
$$D_0^2 z_{m1} + \omega_m^2 z_{m1} = -2D_0D_1z_{m0} - \tilde{\mu}D_0z_{m0} - \hat{\beta}_{cr}(\kappa g_{m2} + f_{m2}\cos 2\sigma T_1)z_{20} \qquad \text{for} \quad m \neq 2 \tag{15}$$

The general solution of Eq. (14) may be written as

$$z_{20} = G_2(T_1)e^{i\omega_1 T_0} + \text{c.c.}$$
$$z_{m0} = G_m(T_1)e^{i\omega_m T_0} + \text{c.c.} \qquad \text{for} \quad m \neq 2 \tag{16}$$

where c.c. denotes the complex conjugate of the preceding term. Substituting Eq. (16) into Eq. (15), one finds that the terms which lead to secular terms (the terms with the coefficient $e^{i\omega_m T_0}$) are eliminated if

$$2i\omega_1(G_1' + ½\tilde{\mu}G_1) + \hat{\beta}_{cr}(\kappa G_{12} + f_{12}\cos 2\sigma T_1)G_2 = 0 \tag{17a}$$

$$2i\omega_1(G_2' + ½\tilde{\mu}G_2) + G_1 = 0 \tag{17b}$$

$$2i\omega_m(G_m' + ½\tilde{\mu}G_m) = 0 \qquad \text{for } m \geq 3 \tag{17c}$$

where the prime denotes a differentiation with respect to T_1. Equation (17c) is independent of the other two, and the general solution of it is

$$G_m = h_m e^{-(\tilde{\mu}/2)T_1} \qquad \text{for} \quad m \geq 3 \tag{18}$$

where the h_m are integration constants. It follows that as time passes, these G_m will die away. In addition, G_1 may be eliminated from Eqs. (17a) and (17b), giving the following equation in G_2 only:

$$G_2'' + \tilde{\mu}G_2' + [¼\tilde{\mu}^2 + (\hat{\beta}_{cr}/4\omega_1^2)(\kappa g_{12} + f_{12}\cos 2\sigma T_1)]G_2 = 0 \tag{19}$$

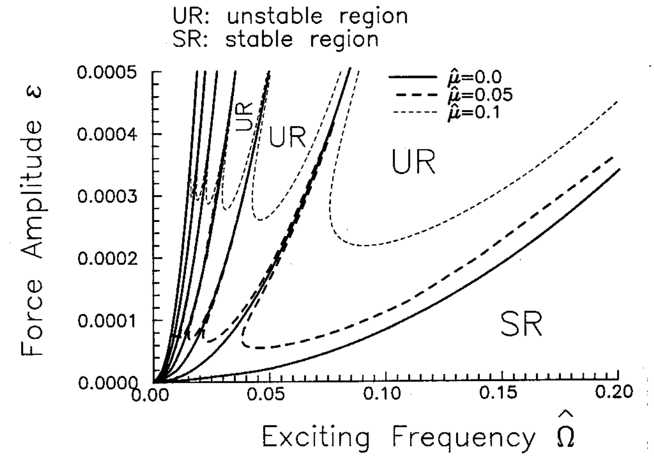

Fig. 2 Transition curves of a cantilever square plate at the critical aerodynamic pressure subjected to an in-plane harmonic force: $\nu = 0.3$, $\hat{\beta}/\hat{\beta}_{cr} = 1.0$.

Equation (19) is a damped Mathieu's equation which possesses no closed-form solution, and the Floquet theory is utilized to analyze the stability of its solution since the theory does not require the coefficient of the nonautonomous term to be small.

IV. Floquet Theory

Setting $\phi = \sigma T_1$ first, Eq. (19) becomes

$$G_2'' + (\tilde{\mu}/\sigma)G_2' + [(\tilde{\mu}^2/4\sigma^2) + (\hat{\beta}_{cr}/4\omega_1^2\sigma^2)(\kappa g_{12} + f_{12}\cos 2\phi)]G_2 = 0 \tag{20}$$

where the prime denotes a differentiation with respect to ϕ. Then, introducing a transformation $G_2 = ue^{-\tilde{\mu}\phi/2\sigma}$, the equation can be reduced to the standard form,

$$u'' + (\delta + \xi \cos 2\phi)u = 0 \tag{21}$$

where the coefficients $\delta = \kappa g_{12}\hat{\beta}_{cr}/4\omega_1^2\sigma^2$ and $\xi = f_{12}\hat{\beta}_{cr}/4\omega_1^2\sigma^2$. By the use of Eq. (13), these two coefficients can be expressed in terms of the original parameters as

$$\delta = \epsilon\kappa g_{12}\hat{\beta}_{cr}/\omega_1^2\hat{\Omega}^2 \qquad \xi = \epsilon f_{12}\hat{\beta}_{cr}/\omega_1^2\hat{\Omega}^2 \tag{22}$$

Since Eq. (21) is a linear, second-order homogeneous differential equation, there exist two linear, nonvanishing independent solutions of this equation, $u_1(\phi)$ and $u_2(\phi)$. It follows that if $u_1(\phi)$ and $u_2(\phi)$ form a fundamental set of solutions of Eq. (21), $u_1(\phi + \pi)$ and $u_2(\phi + \pi)$ must also form a fundamental set of solutions of the same equation. Hence,

$$\begin{aligned} u_1(\phi + \pi) &= p_{11}u_1(\phi) + p_{12}u_2(\phi) \\ u_2(\phi + \pi) &= p_{21}u_1(\phi) + p_{22}u_2(\phi) \end{aligned} \tag{23}$$

where the p_{mn} are the elements of a constant nonsingular matrix $[P]$. According to the Floquet theory, there exists a fundamental set of solutions, v_1 and v_2, having the property

$$\begin{aligned} v_1(\phi + \pi) &= \eta_1 v_1(\phi) \\ v_2(\phi + \pi) &= \eta_2 v_2(\phi) \qquad \text{for} \quad \eta_1 \neq \eta_2 \end{aligned} \tag{24a}$$

or

$$\begin{aligned} v_1(\phi + \pi) &= \eta_1 v_1(\phi) \\ v_2(\phi + \pi) &= \eta_1 v_2(\phi) + {}^{\times} v_1(\phi) \qquad \text{for} \quad \eta_1 = \eta_2 \end{aligned} \tag{24b}$$

where η_i are the eigenvalues of $[P]$ and the superscript $\times$ is 0 or 1 dependent on the Jordan canonical form of the matrix $[P]$. Such solutions are called normal or Floquet solutions. Therefore, the solution of Eq. (20) can be written as

$$G_2 = r_1\chi_1(\phi) + r_2\chi_2(\phi) \tag{25}$$

where the r_i are integration constants, and the fundamental solutions $\chi_i(\phi) = v_i(\phi)e^{-\tilde{\mu}\phi/2\sigma}$.

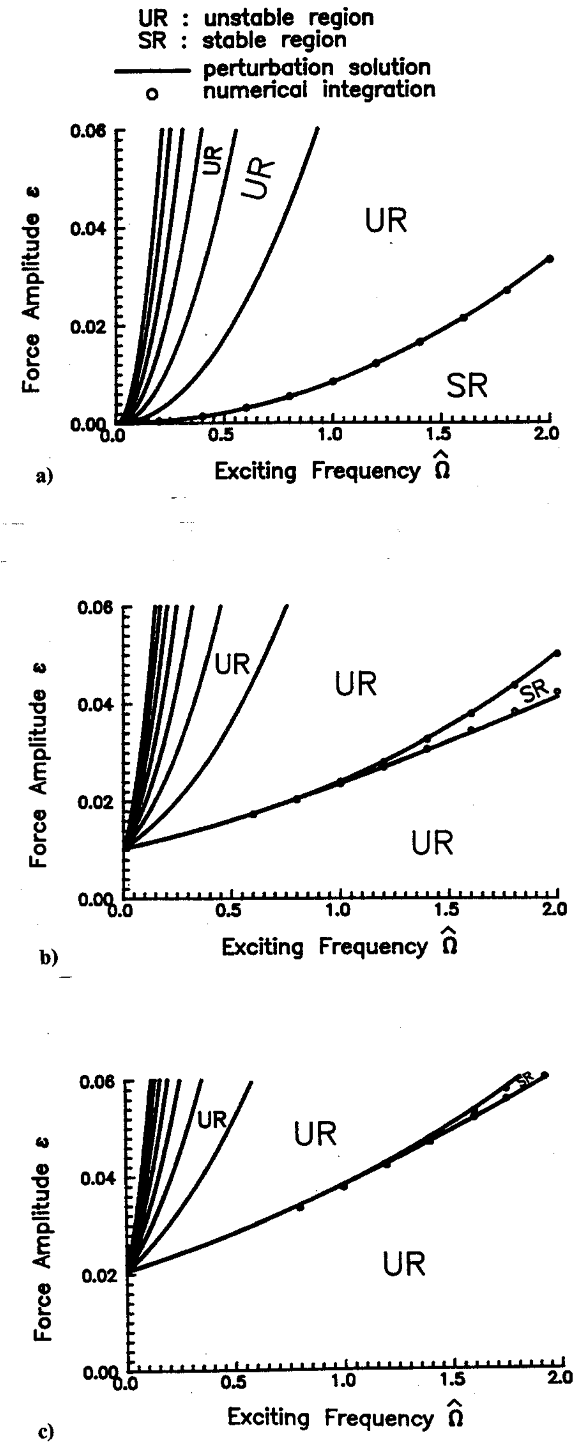

Fig. 3 Transition curves of a fluttered cantilever square plate subjected to an in-plane harmonic force at different values of aerodynamic pressure; $\nu = 0.3$, $\hat{\mu} = 0.05$: a) $\hat{\beta}/\hat{\beta}_{cr} = 1.0$, b) $\hat{\beta}/\hat{\beta}_{cr} = 1.05$, and c) $\hat{\beta}/\hat{\beta}_{cr} = 1.1$.

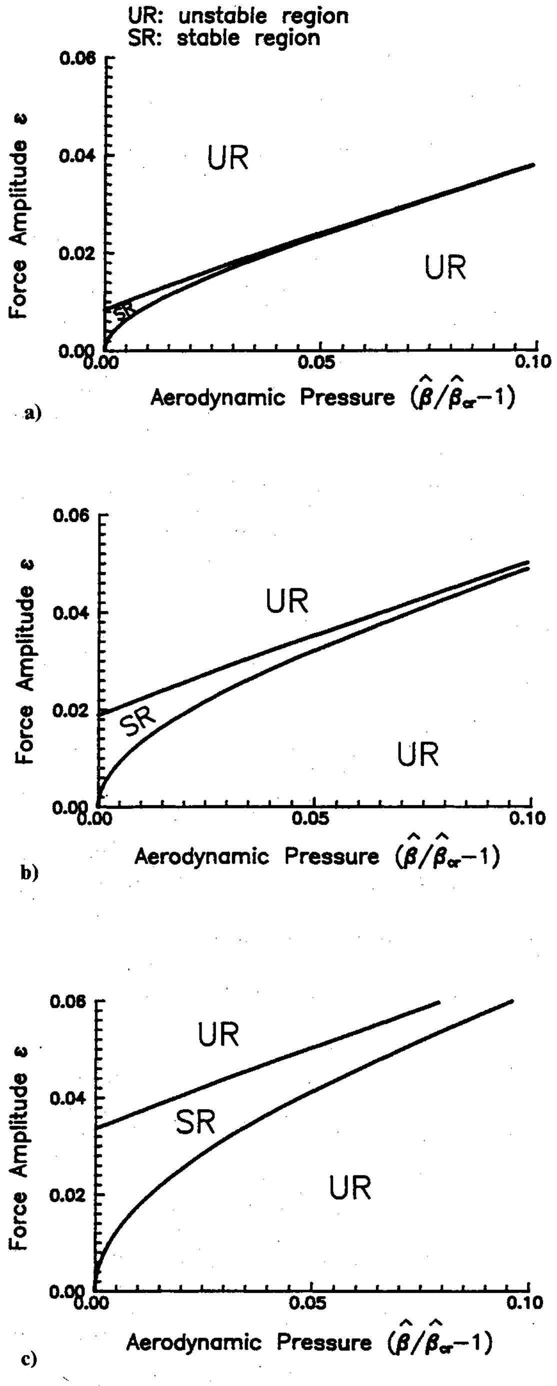

Fig. 4 Transition curves of a fluttered cantilever square plate subjected to an in-plane harmonic force with different exciting frequencies; $\nu = 0.3$, $\hat{\mu} = 0.05$: a) $\hat{\Omega} = 1.0$, b) $\hat{\Omega} = 1.5$, and c) $\hat{\Omega} = 2.0$.

If the $v_i(\phi)$ satisfy Eq. (24a), then

$$\chi_i(\phi + n\pi) = (\eta_i e^{-\bar{\mu}\pi/2\sigma})^n \chi_i(\phi) \tag{26}$$

Consequently, for steady-state motion, i.e., $n \to \infty$,

$$\chi_i(\phi + n\pi) \to \begin{cases} 0, & \text{for} \quad |\eta_i e^{-\bar{\mu}\pi/2\sigma}| \le 1 \\ \infty, & \text{for} \quad |\eta_i e^{-\bar{\mu}\pi/2\sigma}| \ge 1 \end{cases} \tag{27}$$

For $\chi_i \to 0$, the motion is bounded; for $\chi_i \to \infty$, the motion is unbounded. Therefore, the transition curves that separate stable solutions from unstable ones are defined by

$$\max|\eta_i e^{-\bar{\mu}\pi/2\sigma}| = 1, \qquad \text{for} \quad i = 1 \text{ and } 2 \tag{28}$$

If the $v_i(\phi)$ satisfy Eq. (24b), $\chi_1(\phi + n\pi)$ has the same form as shown in Eq. (26). Hence χ_1 is bounded if $|\eta_i e^{-\bar{\mu}\pi/2\sigma}| \le 1$. But

$$\chi_2(\phi + n\pi) = (\eta_i e^{-\bar{\mu}\pi/2\sigma})^n \chi_2(\phi) + n(\eta_i e^{-\bar{\mu}\pi/2\sigma})^{n-1} \chi_1(\phi) \tag{29}$$

Again, χ_2 is bounded if $|\eta_i e^{-\bar{\mu}\pi/2\sigma}| \le 1$. Consequently, the transition curves for this case are still the same as shown in Eq. (28).

To determine the η_i, choose first a suitable fundamental set of solutions $u_1(\phi)$ and $u_2(\phi)$ such that

$$\begin{aligned} u_1(0) &= 1, \qquad & u_1'(0) &= 0 \\ u_2(0) &= 0, \qquad & u_2'(0) &= 1 \end{aligned} \tag{30}$$

Substituting these initial conditions into Eq. (23), the matrix $[P]$ is found to be

$$[P] = \begin{bmatrix} u_1(\pi) & u_1'(\pi) \\ u_2(\pi) & u_2'(\pi) \end{bmatrix} \tag{31}$$

Therefore, the characteristic equation of $[P]$ can be written as

$$\eta^2 - 2s\eta + \Delta = 0 \tag{32}$$

where the constants

$$s = \tfrac{1}{2}[u_1(\pi) + u_2'(\pi)]$$

and

$$\Delta = u_1(\pi)u_2'(\pi) - u_1'(\pi)u_2(\pi)$$

The constant Δ is called the Wronskian determinant of $u_1(\pi)$ and $u_2(\pi)$, which is proved to equal 1 (Ref. 15). Hence, the roots of Eq. (32) are given by

$$\eta_{1,2} = s \pm \sqrt{s^2 - 1} \tag{33}$$

The value of s can be obtained by numerically integrating two linear independent solutions of Eq. (21) having the initial conditions as given in Eq. (30) during the first period of oscillation.

By the use of Eq. (13), the transition curves can be expressed in terms of the original parameters by

$$\max|\eta_i| = e^{\hat{\mu}\pi/\hat{\Omega}}, \qquad \text{for} \quad i = 1 \text{ and } 2 \tag{34}$$

To calculate the transition curves, one must first choose a value for $\hat{\Omega}$, then search for the values of ξ and δ such that they result in a set of η_i which satisfy the condition imposed by Eq. (34), and finally find the values of ϵ and $\epsilon\kappa$ by Eq. (22). Note that $\epsilon\kappa$ is approximately equal to $(\hat{\beta}/\hat{\beta}_{cr}) - 1$ by Eq. (9).

V. Numerical Results and Discussion

Before formally presenting the numerical results for stability studies, convergence studies of the finite element method must be done. According to the previous research done by the authors,[9] 72 triangular elements with 126 degrees of freedom will be used in this work, and the grid work refinement of the finite element model is shown in Fig. 1. With this number of degrees of freedom used, the critical aerodynamic pressure and the corresponding flutter frequency of a cantilever square plate ($\theta = 0$ deg) are calculated to be $\hat{\beta}_{cr} = 58.201$ and $\omega_{fl} = 6.5034$, where the Poisson ratio is taken as 0.3. Both data agree with the results obtained by Srinivasan and Babu[4] within 1%.

In a Strutt diagram, the ϵ-$\hat{\Omega}$ plane is separated into regions of stability and instability by the transition curves. Along these transition curves, at least one of the Floquet solutions is periodic.[15] Figure 2 presents the effect of the aerodynamic damping on the transition curves of a cantilever square plate subjected to the critical aerodynamic pressure and an in-plane harmonic force. In this figure, $\epsilon = Fa^2/\beta_{cr}D$, $\hat{\Omega} = \Omega\sqrt{\rho h a^4/D}$ and $\hat{\mu} = \mu a^2/\sqrt{\rho h D}$. The transition curves are loosely separated at the higher frequency range and are extremely dense when the exciting frequency approaches zero, which makes the locus of the transition curves impossible to be searched. Each curve sprouts from the origin when the aerodynamic damping is neglected, and shrinks upward if the damping is taken into consideration. The regions within the transition curves are unstable, whereas the region outside the curves is stable. Therefore, the effect of the aerodynamic damping is stabilizing. Moreover, the transition curves at the lower frequency range are affected more than those at the higher frequency range. Note that, without the consideration of the aerodynamic damping and the action of the in-plane harmonic force, the system is unstable as the aerodynamic pressure reaches or exceeds its critical value. But with the action of the in-plane harmonic force, the system may become stable at certain suitable combinations of the exciting frequencies and amplitudes even when the aerodynamic pressure exceeds its critical value.

The transition curves of a fluttered cantilever square plate subjected to an in-plane harmonic force at different values of aerodynamic pressure are shown in Fig. 3. Again the transition curves in Figs. 3a and 3b are extremely dense when the exciting frequency approaches zero, which makes the curves impossible to be searched. It is observed that the transition curves move upward and close up toward the lower frequency range as the aerodynamic pressure increases, leaving a smaller stable region. Hence, the effect of the aerodynamic pressure is destabilizing in the postcritical range. Furthermore, to verify the validity of the solution obtained by the perturbation method, some results obtained by direct numerical integration of Eq. (8) are given. As one may see from Fig. 3, the results

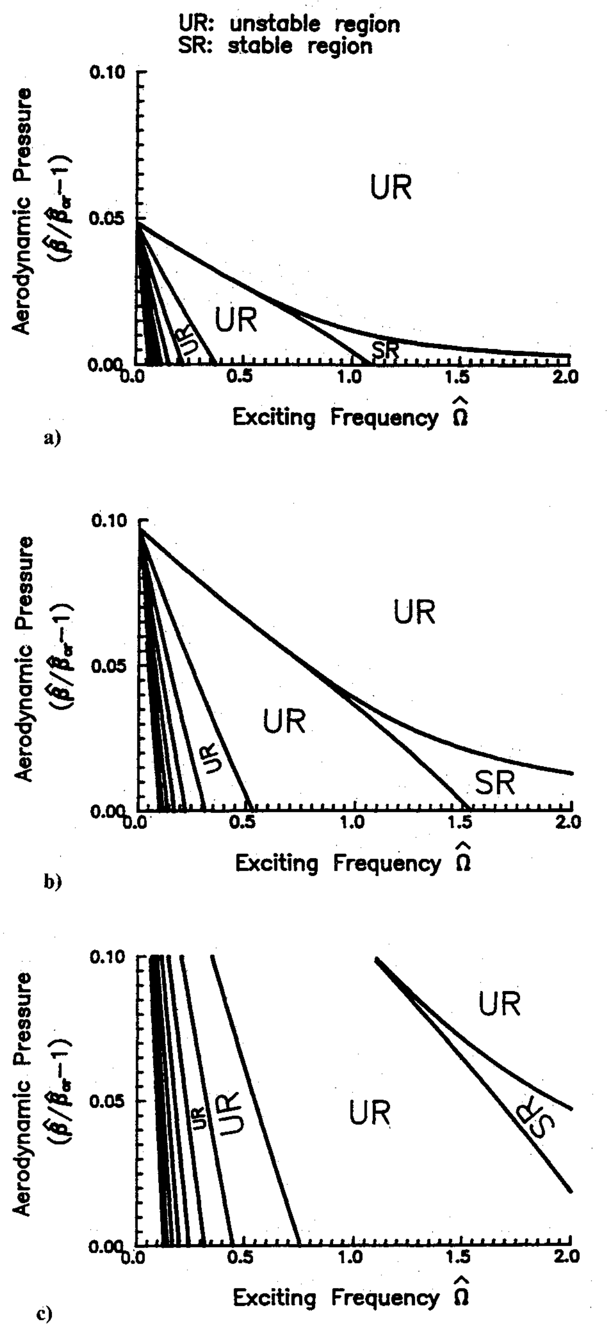

Fig. 5 Transition curves of a fluttered cantilever square plate subjected to an in-plane harmonic force with different amplitudes; $\nu = 0.3$, $\hat{\mu} = 0.05$: a) $\epsilon = 0.01$, b) $\epsilon = 0.02$, and c) $\epsilon = 0.04$.

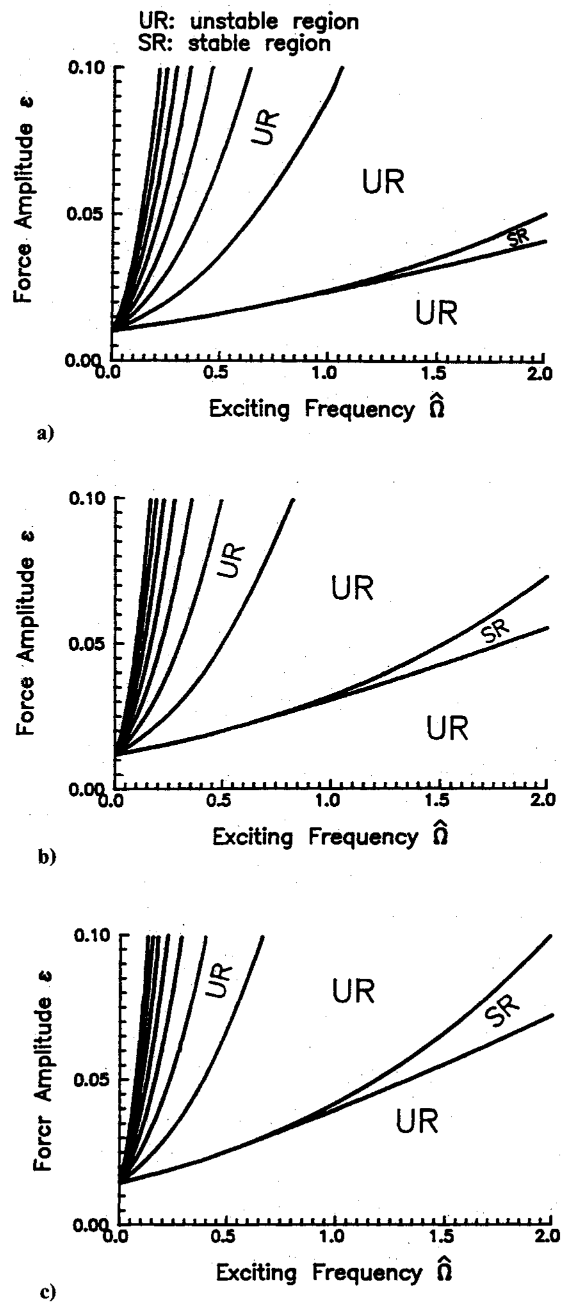

Fig. 6 Transition curves of a cantilever skew plate at a postcritical aerodynamic pressure subjected to an in-plane harmonic force; a/b = 1.0, $\nu = 0.3$, $\hat{\mu} = 0.05$, and $\hat{\beta}/\hat{\beta}_{cr} = 1.05$: a) $\theta = 0$ deg, b) $\theta = 15$ deg, and c) $\theta = 30$ deg.

obtained by these two methods agree closely within the range of parameters shown in this work.

The transition curves of a fluttered cantilever square plate subjected to an in-plane harmonic force with different exciting frequencies are depicted in Fig. 4. The figure reveals that an increase in the exciting frequency shifts the stable region upward and enlarges its size. Hence, the effect of the exciting frequency is stabilizing.

Figure 5 illustrates the transition curves of a fluttered cantilever square plate subjected to an in-plane harmonic force with different amplitudes. The transition curves are thinly scattered at the higher frequency range and are extremely crowded when the exciting frequency approaches zero. It is observed that an increase in the amplitude of the exciting force stretches the transition curves upward, leaving a larger stable region. Consequently, the effect of the amplitude is destabilizing. Moreover, an increase in the amplitude of the exciting force causes the transition curves to spread outwards, which means that the exciting force with a larger amplitude needs a higher exciting frequency to stabilize the system.

Figure 6 presents the effect of changes of the skew angle on the stability boundaries of a fluttered cantilever skew plate subjected to an in-plane harmonic force on the $\hat{\Omega}$-ϵ plane. The figure reveals that the transition curves are pushed upward and closed up toward the lower frequency range as the skew angle becomes larger, giving a larger stable region. Therefore, a plate with a larger skew angle is more stable and needs the exciting force with a larger amplitude but lower frequency to stabilize it. The stability boundaries of a fluttered cantilever skew plate subjected to an in-plane harmonic force on the $\hat{\beta}$-ϵ and $\hat{\Omega}$-$\hat{\beta}$ planes show similar characteristics as already observed in the previous figures.

VI. Conclusions

The dynamic stability of a cantilever skew plate subjected to an aerodynamic force with the magnitude exceeding its critical value and acted on simultaneously by an in-plane harmonic force was studied in this paper. The effects of system parameters on the changes of the transition curves of the system were investigated, and the following conclusions are obtained.

1) When the aerodynamic pressure exceeds its critical value, the plate may remain stable under the action of the in-plane harmonic force at certain combinations of the amplitude and the exciting frequency.

2) The effects of the exciting frequency and amplitude of the in-plane harmonic force are both stabilizing.

3) An increase in the aerodynamic pressure destabilizes the system in the postcritical range, and an increase in the aerodynamic damping stabilizes the system.

4) A plate with a larger skew angle is more stable.

Acknowledgment

This work was sponsored by the National Science Council of the Republic of China under Grant NSC80-0401-E011-07.

References

[1]Fung, Y. C., "Some Recent Contributions to Panel Flutter Research," *AIAA Journal,* Vol. 1, No. 4, 1963, pp. 898–909.

[2]Bisplinghoff, R. L., and Ashley, H., *Principles of Aeroelasticity,* Wiley, New York, 1962, p. 416.

[3]Durvasula, S., "Flutter of Simply Supported, Parallelogrammic, Flat Panels in Supersonic Flow," *AIAA Journal,* Vol. 5, 1967, pp. 1668–1673.

[4]Srinivasan, R. S., and Babu, B. J. C., "Flutter Analysis of Cantilevered Quadrilateral Plates," *Journal of Sound and Vibration,* Vol. 98, No. 1, 1985, pp. 45–53.

[5]Olson, M. D., "Flutter Solutions Using Finite Elements," *AIAA Journal,* Vol. 8, No. 4, 1970, pp. 747–752.

[6]Ibrahim, R. A., Orono, P. O., and Madaboosi, S. R., "Stochastic Flutter of a Panel Subjected to Random In-Plane Forces, Part I: Two Mode Interaction," *AIAA Journal,* Vol. 24, No. 4, 1990, pp. 694–702.

[7]Dugundji, J., "Theoretical Considerations of Panel Flutter at High Supersonic Mach Numbers," *AIAA Journal,* Vol. 4, No. 7, 1966, pp. 1257–1266.

[8]Sander, G., Bon, C., and Geradin, M., "Finite Element Analysis of Supersonic Panel Flutter," *Journal for Numerical Methods in Engineering,* Vol. 7, 1973, pp. 379–394.

[9]Young, T. H., and Chen, F. Y., "Stability of Skew Plates Subjected to Aerodynamic and In-Plane Exciting Forces," *Journal of Sound and Vibration,* Vol. 167, No. 2, 1993 (to be published).

[10]Fu, F. C. L., and Namet-Nasser, S., "Stability of Solution of Systems of Differential Equations with Harmonic Coefficients," *AIAA Journal,* Vol. 10, No. 1, 1972, pp. 30–36.

[11]Fu, F. C. L., and Namet-Nasser, S., "Response and Stability of Linear Dynamic Systems with Many Degrees of Freedom Subjected to Nonconservative and Harmonic Forces," *Journal of Applied Mechanics,* Vol. 42, No. 2, 1975, pp. 458–463.

[12]Zienkiewicz, O. C., *The Finite Element Method,* McGraw-Hill, Maidenhead, Berkshire, England, UK, 1977, pp. 241–244.

[13]Franklin, J. N., *Matrix Theory,* Prentice-Hall, Englewood Cliffs, NJ, 1968, pp. 125–131.

[14]Meirovitch, L., *Computational Methods in Structural Dynamics,* Sijthoff and Noordhoff, Rijn, The Netherlands, 1980, pp. 204–208.

[15]Nayfeh, A. H., and Mook, D. T., *Nonlinear Oscillations,* Wiley, New York, 1979, pp. 273–331.